

## Competitive adsorption of Dibutyl phthalate (DBP) and Di(2-ethylhexyl) phthalate (DEHP) onto fresh and oxidized corncob biochar

Chemosphere

Abdoul Magid, Abdoul Salam Issiaka; Islam, Md Shafiqul; Chen, Yali; Weng, Liping; Sun, Yang et al  
<https://doi.org/10.1016/j.chemosphere.2021.130639>

This publication is made publicly available in the institutional repository of Wageningen University and Research, under the terms of article 25fa of the Dutch Copyright Act, also known as the Amendment Taverne. This has been done with explicit consent by the author.

Article 25fa states that the author of a short scientific work funded either wholly or partially by Dutch public funds is entitled to make that work publicly available for no consideration following a reasonable period of time after the work was first published, provided that clear reference is made to the source of the first publication of the work.

This publication is distributed under The Association of Universities in the Netherlands (VSNU) 'Article 25fa implementation' project. In this project research outputs of researchers employed by Dutch Universities that comply with the legal requirements of Article 25fa of the Dutch Copyright Act are distributed online and free of cost or other barriers in institutional repositories. Research outputs are distributed six months after their first online publication in the original published version and with proper attribution to the source of the original publication.

You are permitted to download and use the publication for personal purposes. All rights remain with the author(s) and / or copyright owner(s) of this work. Any use of the publication or parts of it other than authorised under article 25fa of the Dutch Copyright act is prohibited. Wageningen University & Research and the author(s) of this publication shall not be held responsible or liable for any damages resulting from your (re)use of this publication.

For questions regarding the public availability of this publication please contact [openscience.library@wur.nl](mailto:openscience.library@wur.nl)



## Competitive adsorption of Dibutyl phthalate (DBP) and Di(2-ethylhexyl) phthalate (DEHP) onto fresh and oxidized corncob biochar



Abdoul Salam Issiaka Abdoul Magid <sup>a</sup>, Md Shafiqul Islam <sup>a</sup>, Yali Chen <sup>a, \*</sup>, Liping Weng <sup>a, b</sup>, Yang Sun <sup>a</sup>, Xingping Chang <sup>a</sup>, Bin Zhou <sup>a</sup>, Jie Ma <sup>a</sup>, Yongtao Li <sup>c, d</sup>

<sup>a</sup> Agro-Environmental Protection Institute, Ministry of Agriculture and Rural Affairs / Key Laboratory of Original Agro-Environmental Pollution Prevention and Control, MARA / Tianjin Key Laboratory of Agro-Environment and Agro-Product Safety, Tianjin 300191, PR China

<sup>b</sup> Department of Soil Quality, Wageningen University, P.O. Box 47, 6700, AA, Wageningen, the Netherlands

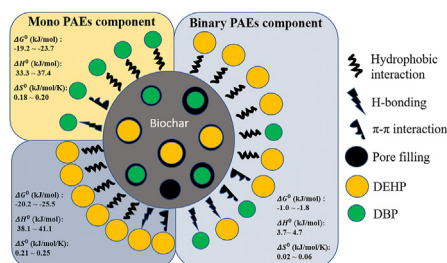
<sup>c</sup> College of Natural Resources and Environment, South China Agricultural University, Guangzhou, 510642, PR China

<sup>d</sup> College of Resource and Environmental Engineering, Jiangxi University of Science and Technology, Ganzhou Jiangxi, 341000, PR China

### HIGHLIGHTS

- The biochar showed significantly greater adsorption capacity for DEHP than for DBP.
- Sorption capacity of oxidized biochar for PAEs increased due to the enhancement of surface complexation.
- Competition between DEHP and DBP in their adsorption to the biochar was observed.
- The stronger adsorption of DEHP than DBP resulted from its stronger hydrophobic interaction with biochar.

### GRAPHICAL ABSTRACT



### ARTICLE INFO

#### Article history:

Received 28 November 2020

Received in revised form

23 March 2021

Accepted 18 April 2021

Available online 23 April 2021

Handling Editor: Junfeng Niu

#### Keywords:

Competitive adsorption  
Biochar  
Phthalates  
Mechanism

### ABSTRACT

Phthalates (PAEs) often exist simultaneously in contaminated soil and wastewater systems, and their adsorption to biochar might impact their behavior in the environment. So far, the competitive adsorption of PAEs to biochar has not been reported. In this study, the competitive adsorption of Dibutyl phthalate (DBP) and Di(2-ethylhexyl) phthalate (DEHP) on corncob biochar (fresh and oxidized) was investigated, and experiments of kinetics, isotherms, and thermodynamics were conducted. Langmuir and Freundlich models, pseudo-first-order and second-order kinetic models were used to simulate the experimental data. In the mono PAEs component systems, the biochar showed significantly greater adsorption capacity for DEHP (11.8–16.16 mg g<sup>-1</sup>) than for DBP (9.86–13.2 mg g<sup>-1</sup>). The oxidized biochar has higher adsorption capacities than the fresh one. Moreover, a fast adsorption rate for DBP was observed, which can be attributed to the smaller size and shorter carbon chains in the DBP molecule, resulting in faster diffusion into the biochar pores. In the binary PAEs component systems, competition between DEHP and DBP in their adsorption to the biochars was observed, and DEHP (11.7–15.0 mg g<sup>-1</sup>) was preferred over DBP (3.4–7.9 mg g<sup>-1</sup>). The stronger adsorption of DEHP can be explained by stronger hydrophobic interaction with biochar. Compared to DBP, DEHP has a high octanol-water partition coefficient (logK<sub>ow</sub>) and low water solubility. The positive entropy ( $\Delta S^0$ ) and enthalpy ( $\Delta H^0$ ) values for the adsorption of both

\* Corresponding author.

E-mail address: [chenyali@caas.cn](mailto:chenyali@caas.cn) (Y. Chen).

DEHP and DBP further indicated that hydrophobic interaction played an important role, even though H-bonds and  $\pi$ - $\pi$  interactions could also be involved.

© 2021 Elsevier Ltd. All rights reserved.

## 1. Introduction

Phthalates (PAEs) are a class of organic compounds commonly used as plasticizers in polyvinyl chloride (PVC). Since PAEs are physically associated with the PVC polymer, they can be leached from the PVC products during or after use (Staples et al., 1997). Recent investigations show that the world production of PAEs is around 6 million tons per year, and a large fraction of these substances can potentially be released into the environment (air, sediment, natural water, wastewater, and soils) (Zhang et al., 2014). Because of the enormous volumes of PVC produced, PAEs have become sources of pollution in the environment. For example, some of the PAEs, e.g., Dibutyl phthalate (DBP); Di(2-Ethylhexyl) phthalate (DEHP); Butyl Benzyl phthalate (BBP) and Diethyl phthalate (DEP), have bioaccumulation potentials and are considered endocrine-disrupting chemicals and classified by many countries as "priority pollutants" (Lu et al., 2009). Studies have shown that PAEs are acutely or chronically toxic to organisms in aquatic environments (Chung and Chen, 2009). On humans, PAEs exert harmful effects, such as disrupting the male reproductive system and being carcinogenic (Chang et al., 2004; Foster et al., 2000). In the environment, PAEs can adsorb to many matrices (soil and organic sediments) (Gao et al., 2013; Jin et al., 2015). The adsorption of PAEs strongly influences their behavior in the environment, such as their mobility, bioavailability, and stability (Li et al., 2006; Qin et al., 2018; Xiang et al., 2019).

Biochar is a product derived from thermochemical biomass treatment under a minimal oxygen environment (Ahmad et al., 2014; Kookana, 2010). There is a growing interest in applying biochar as a soil amendment to improve agricultural soils' quality. Biochar can decrease soil acidity and increases soil fertility, soil porosity, and water retention (Chen et al., 2011; Huang et al., 2017), and consequently improve plant growth and land productivity. Other potential effects of biochar amendments in soil include sequestration of carbon, decreases greenhouse gas emissions, sorption, and deactivation of agrochemicals (Cayuela et al., 2014; Jeffery et al., 2011; Sánchez-García et al., 2015). Biochars are capable of binding pollutants to protect the environment (Beesley et al., 2011). Owing to its large surface area and high porosity, biochar can adsorb different types of inorganic and organic chemicals (Chen et al., 2019; Ghaffar and Abbas, 2016; Herath et al., 2016; Jin et al., 2014; Qureshi et al., 2016). For heavy metals, the application of bamboo and rice straw biochar could immobilize Zn, Pb, Cd, and Cu in soil and reduce their bioavailability (Lu et al., 2017). In contrast, Zhou et al. (2020) investigated pinewood and bamboo biochar for Cr removal. With regards to organic pollutants, corn straw biochar was tested for herbicide removal and its sorption capacity  $\log K_{OC}$  values ranged from  $10^{3.298}$ – $10^{4.919}$  L/kg (Zhang et al., 2011), whereas bamboo biochar was studied for antibiotics removal, and their results showed that more than 99% of fluoroquinolone antibiotics was removed from synthetic wastewater through adsorption (Wang et al., 2015).

There are different types of PAEs commonly found in the environment, and they show variations in properties such as aqueous solubility, hydrophobicity, and molecular size. DBP and DEHP are the most frequently reported PAEs in environmental samples (Peijnenburg and Struijs, 2006). Because of their prevalence in the

environment, it is meaningful to compare DBP and DEHP's adsorption behavior. For example, the surface molecularly imprinted polymer adsorbed more DEHP than DBP and some other phthalates (Dimethyl phthalate, Di-n-octyl phthalate and DEP), and the molecular volume and dimensional structure of the polymer and PAEs determined the selectivity of DEHP (Yang et al., 2015). Besides, DEHP was adsorbed more than DBP on magnetic and non-magnetic chitosan/PVA hydrogels, and the adsorption processes were governed by hydrogen bonding, complexation, and hydrophobic interactions (Qureshi et al., 2016). Although studies showed that PAEs, including DBP and DEHP, can adsorb to biochar (Chen et al., 2019; Ghaffar and Abbas, 2016; He et al., 2016), the adsorption behavior of DBP and DEHP on biochar and their possible competition in the adsorption have not been investigated systematically.

In this study, biochar from corncob was produced at different pyrolysis temperatures (700 °C and 900 °C) and then characterized. Chemical oxidation was used to mimic the "aging" of biochar in the environment. DBP and DEHP's adsorption on fresh and oxidized corncob biochar were investigated in mono and binary PAEs component systems under conditions similar to the natural environment. The main aim of this study is to: (1) investigate the competitive adsorption of DBP and DEHP by fresh and oxidized corncob biochar; (2) examine the involved adsorption mechanisms. To the best of our knowledge, this is the first study to investigate the competitive adsorption behaviors of DBP and DEHP onto biochar. The findings of this research would advance our understanding in studying the environmental fate of PAEs in the presence of biochar in soils and water.

## 2. Materials and methods

### 2.1. Chemicals

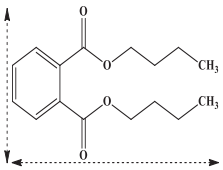
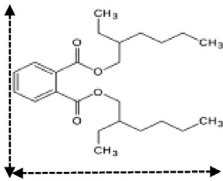
Analytical grade reagents of DBP ( $\geq 97.0\%$ ) and DEHP ( $\geq 98.0\%$ ) were obtained from ANPEL Laboratory Technologies (Shanghai, China). Table 1 presents the selected physico-chemical properties of DBP and DEHP. Ultrapure water was made using an Arrium® mini pro-VF Ultrapure Water System. During the experiment, no plastic equipment was used to prevent contamination.

### 2.2. Preparation of fresh and oxidized biochar

Corn cob was obtained from a local farm in Wuqing District, Tianjin, China. The feedstock was air-dried and stored in sealed containers. Biochar was produced from corncob in a muffle furnace under limited oxygen conditions at 700 °C (referred to as B700) and 900 °C (referred to as B900) for 2 h. The obtained biochar was gently crushed and sieved to <0.15 mm.

A mixture of  $\text{HNO}_3$ – $\text{H}_2\text{SO}_4$  was selected to oxidize the biochar (B700 and B900) according to a modified method (Qian and Chen, 2013). Several studies have demonstrated that biochar treated with a potent oxidizing agent (e.g.,  $\text{HNO}_3/\text{H}_2\text{SO}_4$ ,  $\text{HNO}_3$ ,  $\text{HF}/\text{HNO}_3$ ,  $\text{KMnO}_4$ ,  $\text{H}_2\text{O}_2$ , or  $\text{NaClO}$ ) creates charged and hydrophilic surface functional groups, increases their colloidal stability and mobility, and enhances its sorption capacities (Cho et al., 2010). Briefly, the  $\text{HNO}_3$ – $\text{H}_2\text{SO}_4$  mixture (1:3, v/v) was diluted with deionized water

**Table 1**  
Selected physico-chemical properties of the phthalic acid esters (PAEs).

| Structure                                                                         | Chemicals                  | Abb. | MF <sup>ac</sup>                               | M <sup>ab</sup> | AS <sup>bc</sup> | r <sup>ac</sup> | LogK <sub>ow</sub> <sup>ab</sup> | ML <sup>de</sup> | MW <sup>de</sup> |
|-----------------------------------------------------------------------------------|----------------------------|------|------------------------------------------------|-----------------|------------------|-----------------|----------------------------------|------------------|------------------|
|  | Dibutyl phthalate          | DBP  | C <sub>16</sub> H <sub>18</sub> O <sub>4</sub> | 278             | 11.2             | 1.05            | 4.61                             | 1.265            | 1.229            |
|  | Di(2-ethylhexyl) phthalate | DEHP | C <sub>24</sub> H <sub>38</sub> O <sub>4</sub> | 391             | 0.003            | 0.99            | 7.5                              | 1.388            | 1.032            |

MF: molecular formula, M: molar mass (g mol<sup>-1</sup>), AS: Aqueous solubility weight (mg L<sup>-1</sup>), r: density (g cm<sup>-3</sup>), Log K<sub>ow</sub>: octanol/water partition constant, ML: Molecular length, MW: Molecular width, <sup>a</sup> From Ref. (Chaffar et al., 2015), <sup>b</sup> From Ref. (Liu et al., 2014), <sup>c</sup> From Ref. (German, 2014), <sup>d</sup> From Ref. (Chen et al., 2019), <sup>e</sup> From Ref (Chaffar et al., 2017).

to 5%, and then 5 g of B700 or B900 was immersed in 400 mL of the 5% HNO<sub>3</sub>–H<sub>2</sub>SO<sub>4</sub> solution and maintained for 6 h at 80 °C. The oxidized biochar was washed repeatedly with deionized water and then drained over a 0.45 μm membrane. The oxidized biochar samples were designated as AB700 and AB900.

### 2.3. Characterization of biochar

Suspensions of biochar were prepared by adding 0.1 g biochar to 10 mL ultra-pure water, which was shaken at 250 rpm for 24 h; the pH in the supernatant was measured with a pH meter (Toledo, Shanghai). A scanning electron microscope (SEM-Hitachi SU-1510) was used to show the surface morphology of the materials. An elemental analyzer (Vario EL cube SN-19103023) was used to evaluate proportions of carbon, oxygen, hydrogen, nitrogen, and sulfur of biochar through dry combustion. Ash content was determined after heating the biochar to 750 °C. The specific surface area (SSA) and pore size of each biochar were determined using the BET-N<sub>2</sub> adsorption method (Micro metrics Instrument Corporation, TriStar II 3020 Version 3.02 Serial 1421). The surface functional groups on biochar were analyzed with the Fourier transform infrared (FTIR) spectra in the range of 4000–400 cm<sup>-1</sup> (Thermo Nicolet Corporation, Nexus870). The C- and O-containing groups on the biochar surface were determined using the X-ray photoelectron spectroscopy (XPS) (Thermo ESCALAB 250Xi XPS Method).

### 2.4. Adsorption experiments

Standard DBP and DEHP were separately dissolved into methanol (50 g L<sup>-1</sup>) as stock solutions. All batch adsorption experiments were carried out in 30 mL glass vials with Teflon screw caps. The headspaces of all vials were held to avoid the loss of PAEs. Different series of adsorption experiments were carried out. (i) adsorption edge at pH 3–10, (ii) adsorption isotherms at pH 7 under three temperatures (288 K, 298 K, and 308 K), (iii) adsorption kinetics at pH 7. In all the experiments, 30 mg of biochar (B700, B900, AB700, AB900) was added to each vial. Diluted stock solutions of DBP and DEHP were added to the vial individually or together. The suspensions' pH was adjusted to desired levels by adding 0.01 mol L<sup>-1</sup> HNO<sub>3</sub> or NaOH. In the adsorption edge and adsorption kinetic experiment (experiment i & iii), the concentrations of DBP and DEHP were 60 mg L<sup>-1</sup>; in the adsorption isotherm experiment, the

concentrations of DBP and DEHP were in the range of 10–60 mg L<sup>-1</sup>. The proportion of methanol was kept below 0.10% (v/v) to minimize the co-solvent effect. In all the experiments, the solution of NaCl was added to a final concentration of 0.01 mol L<sup>-1</sup>. The final volume of the solution in each vial was 10 mL, and the final content of biochar was 3 g L<sup>-1</sup>. All the suspensions were shaken at 180 rpm at room temperature for 48 h (experiment i and ii) or up to 72 h (experiment iii). The pH in the suspensions was measured; after that, the suspensions were filtered over 0.45 μm membrane. In the filtrates, the concentrations of DBP and DEHP were measured. In the kinetic adsorption experiment, at various time intervals between 15 min and 72 h, samples were taken and treated in the same way as above.

The amount of PAEs removed by biochar, *Q* (mg g<sup>-1</sup>), was derived from the difference between the initial and end PAEs concentrations in solution:

$$Q = \frac{(C_i - C_e)V}{m} \quad (\text{Eq. 1})$$

where *C<sub>i</sub>* (mg L<sup>-1</sup>) and *C<sub>e</sub>* (mg L<sup>-1</sup>) represent the initial and equilibrium concentrations of the PAEs (DBP and DEHP) in solution, respectively, and *V* (L) is the volume of the solution, and *m* (g) is the mass of biochar.

### 2.5. DBP and DEHP analysis

The DBP and DEHP in solution were measured by Ultra Performance Liquid Chromatography (UPLC, LC-20AD, Shimadzu Kyoto, Japan) equipped with a reversed-phase C18 analytical column (1.7 μm, 2.1 mm × 50 mm) and photodiode array detector. The mobile phase was a mixture of acetonitrile and deionized water (v:v = 8:2). The measurement conditions were as follows: flow rate 1 mL min<sup>-1</sup>, injection volume 10 μL, column temperature 35 °C, detection wavelength 224 nm. The retention time of DBP and DEHP was 5.2 and 6.5 min, respectively. The concentrations of DBP and DEHP were calculated using the peak area-concentration standard curve (Figure S1).

**Table 2**  
Characterization of fresh (B700 and B900) and oxidized biochar (AB700 and AB900).

| Biochar | pH  | C (%) | H (%) | N (%) | O (%) | O/C  | H/C  | (N + O)/C (%) | Ash (%) | SA (m <sup>2</sup> g <sup>-1</sup> ) | PV (cm <sup>3</sup> g <sup>-1</sup> ) | PS (nm) |
|---------|-----|-------|-------|-------|-------|------|------|---------------|---------|--------------------------------------|---------------------------------------|---------|
| B700    | 9.6 | 79.9  | 2.0   | 0.7   | 13.9  | 0.13 | 0.30 | 0.14          | 3.5     | 34.51                                | 0.06                                  | 9.12    |
| AB700   | 3.6 | 72.9  | 1.9   | 1.67  | 20.29 | 0.21 | 0.31 | 0.23          | 3.24    | 48.18                                | 0.11                                  | 8.82    |
| B900    | 9.7 | 81.2  | 1.9   | 0.67  | 13.7  | 0.12 | 0.28 | 0.13          | 2.53    | 36.28                                | 0.06                                  | 9.79    |
| AB900   | 3.9 | 65.3  | 1.6   | 1.45  | 29.26 | 0.34 | 0.29 | 0.36          | 2.39    | 60.83                                | 0.13                                  | 9.09    |

SA: Surface area; PV: Pore volume; PS: Pore size.

### 3. Results

#### 3.1. Characteristics of biochar

The elemental compositions of the fresh biochar (B700 and B900) and their oxidized equivalents (AB700 and AB900) were presented in Table 2. The increase in pyrolysis temperature from 700 °C to 900 °C accounted for slightly increased C content in the fresh biochar. In contrast, O and H contents were slightly decreased, indicating cumulative carbonization following decarboxylation and dehydration during pyrolysis (Ghaffar and Abbas, 2016). Chemical oxidation significantly influenced the bulk composition of biochar, resulted in an increase in O and N contents and a decrease in C and H contents. After oxidation, the O/C ratio of biochar increased by about 61.5% and 183.3% under pyrolysis temperatures of 700 °C and 900 °C, respectively. The pH and ash content decreased considerably after oxidation because the alkaline components were eliminated when AB700 and AB900 were washed with water during the oxidation treatment (Qian and Chen, 2013).

The SEM images showed the surface morphology and structure of the four biochar materials (Fig. 1). It was clear that with the

increase of pyrolysis temperature, more large pores (>1 μm) appeared in the materials (B700 and B900). This was because the lignocellulosic content was decomposed at high temperatures, accompanied by volatile compounds' evaporation, leaving samples with well-formed pores (Jing et al., 2018). The BET-N<sub>2</sub> determined specific surface area increased by about 5%, and the pore volume (pore size < 100 nm) and pore size increased by about 15% and 7.3%, respectively, in B900 in comparison to B700 (Table 2). Compared to the non-oxidized samples, the clean appearance and high porosity of the oxidized biochars (AB700 and AB900) were visible (Fig. 1). The specific surface area and pore volume (pore size < 100 nm) of oxidized biochar were higher than the fresh biochar (Table 2), increased by about 39.7–67.5% and 83.3–85.7%, respectively, because some of the organic matter was decomposed and consumed during the oxidation, causing pore expansion and forming more pore structure, leading to larger surface area (Zhang et al., 2014).

The FTIR spectra for B700, B900, AB700, and AB900 were obtained in the range of 400–4000 cm<sup>-1</sup> (Figure S2). The broadband at about 3438 cm<sup>-1</sup> was correlated to the –OH group, suggesting hydroxyl group was present on the biochar sample surface (Wang

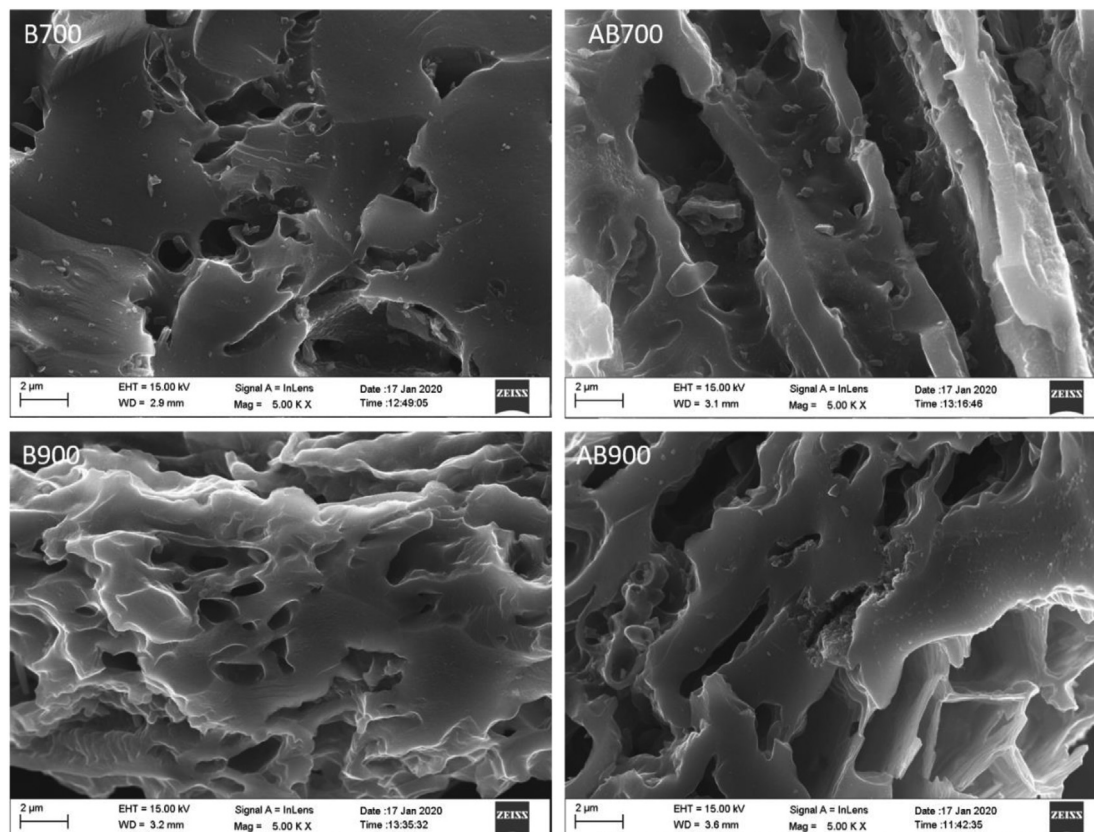


**Fig. 1.** SEM of fresh (B700, B900) and oxidized (AB700, AB900) biochar.

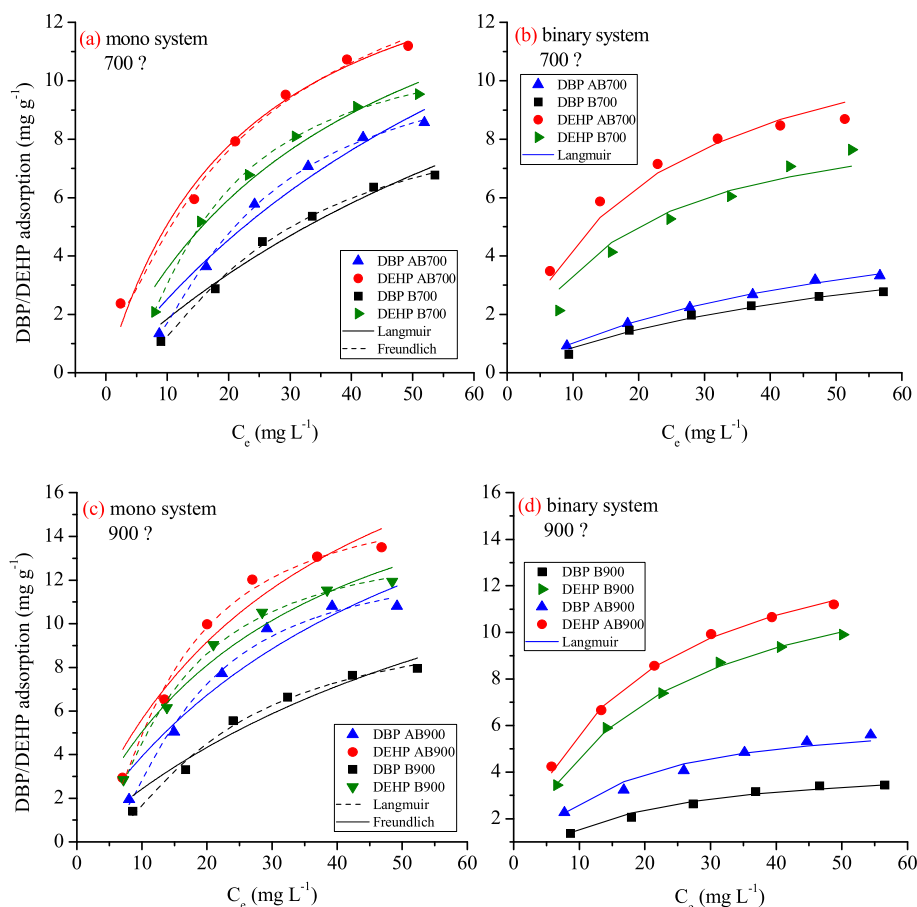


Fig. 2. Adsorption isotherms of DBP and DEHP under mono (a, c) and binary (b, d) conditions.

et al., 2013). The characteristic peak at about  $1597\text{ cm}^{-1}$  was linked primarily to ester  $\text{C}=\text{O}$  stretching vibrations (Gan et al., 2015). The peak at about  $1381\text{ cm}^{-1}$  was associated with  $-\text{COO}$  group, and the  $\text{C}-\text{O}$  bending vibration was assigned to the band at wavenumber near  $1114\text{ cm}^{-1}$  (Dong et al., 2017). Results indicate that biochar's surface contains more oxygen-containing surface groups after oxidation, especially the  $-\text{OH}$  and  $\text{C}-\text{O}$  groups.

### 3.2. Adsorption isotherms of DBP and DEHP in mono and binary component systems

The adsorption isotherms of DBP and DEHP to the biochar materials in mono and binary PAEs component systems were investigated. From Fig. 2, it can be seen that the amount of DBP and DEHP adsorbed at equilibrium ( $Q_e$ ) increased with the solution concentration ( $C_e$ ) and the isotherms are non-linear. No adsorption plateau was reached in the concentration range studied.

The Langmuir, Freundlich, two-component Langmuir models were used to describe the experimental data. The Langmuir, Freundlich, and two-component Langmuir model's linear equation was presented in Supplementary Material S3.

In the mono component systems, DEHP adsorption on each of the biochar materials was generally stronger than DBP (Fig. 2a and c). Based on the maximum adsorbed amount measured, the

adsorption capacity of the biochar for DBP followed the order of  $\text{AB900} > \text{AB700} > \text{B900} > \text{B700}$ , whereas for DEHP the order was  $\text{AB900} > \text{B900} \approx \text{AB700} > \text{B700}$ . The maximum adsorption was found in AB900 for both DEHP ( $16.2\text{ mg g}^{-1}$ ) and DBP ( $13.2\text{ mg g}^{-1}$ ). The Langmuir and Freundlich model calculations (lines) were compared to the measurements (symbols) in Fig. 2a and c, and the optimized model constants were provided in Table 3. The Freundlich model could well describe the adsorption of DBP and DEHP ( $R^2 = 0.98\text{--}0.99$ ). The goodness of fit to the Langmuir model was slightly less ( $R^2 = 0.91\text{--}0.96$ ) but still acceptable. Because the adsorption isotherms did not reach a clear plateau, the  $Q_{max}$  fitted had large uncertainties.

Compared to the mono PAEs component systems, in the binary systems, the DEHP adsorption on biochar was slightly inhibited by DBP addition, while DBP adsorption was more severely reduced (Fig. 2b and d). For example, the DBP adsorption in the mono component system on B900 and AB900 was  $8.0\text{ mg g}^{-1}$  and  $10.8\text{ mg g}^{-1}$  with the initial DBP concentration of  $60\text{ mg L}^{-1}$ . It was decreased to respectively  $3.4\text{ mg g}^{-1}$  and  $5.6\text{ mg g}^{-1}$  in the binary PAEs component systems in the presence of  $60\text{ mg L}^{-1}$  DEHP (Fig. 2). On the contrary, under the same situations, the adsorption amounts of DEHP on B900 and AB900 were decreased from  $11.9\text{ mg g}^{-1}$  and  $13.5\text{ mg g}^{-1}$  to  $9.9\text{ mg g}^{-1}$  and  $11.2\text{ mg g}^{-1}$ , respectively. These results indicated the presence of competition

**Table 3**  
Fitting results of DBP and DEHP adsorption on biochar based on mono component Langmuir and Freundlich models, and two component Langmuir model.

|         |         | Mono component             |                        |       |                        |      |       |
|---------|---------|----------------------------|------------------------|-------|------------------------|------|-------|
| Sorbate | Biochar | Langmuir Isotherm          |                        |       | Freundlich Isotherm    |      |       |
|         |         | $Q_{max}$ ( $mg\ g^{-1}$ ) | $K_L$ ( $L\ mg^{-1}$ ) | $R^2$ | $K_f$ ( $L\ mg^{-1}$ ) | $n$  | $R^2$ |
| DBP     | B700    | 20.23                      | 0.01                   | 0.96  | 9.86                   | 1.36 | 0.99  |
|         | AB700   | 22.9                       | 0.012                  | 0.94  | 11.25                  | 1.53 | 0.99  |
|         | B900    | 20.26                      | 0.01                   | 0.94  | 10.67                  | 1.48 | 0.98  |
|         | AB900   | 23.88                      | 0.02                   | 0.91  | 13.21                  | 1.74 | 0.98  |
| DEHP    | B700    | 17.63                      | 0.02                   | 0.96  | 11.79                  | 1.48 | 0.99  |
|         | AB700   | 16.5                       | 0.04                   | 0.97  | 13.38                  | 0.98 | 0.99  |
|         | B900    | 20.59                      | 0.03                   | 0.95  | 14.26                  | 1.57 | 0.99  |
|         | AB900   | 24.85                      | 0.03                   | 0.93  | 16.16                  | 1.64 | 0.98  |

|          |         | Binary component                |                             |                                      |       |
|----------|---------|---------------------------------|-----------------------------|--------------------------------------|-------|
| Sorbate  | Biochar | Two component Langmuir isotherm |                             |                                      | $R^2$ |
|          |         | $K_{DBP}$ ( $L\ mg^{-1}$ )      | $K_{DEHP}$ ( $L\ mg^{-1}$ ) | $Q_{max(DBP-DEHP)}$ ( $mg\ g^{-1}$ ) |       |
| DBP-DEHP | B700    | 0.006                           | 0.019                       | 15.31                                | 0.985 |
| DBP-DEHP | AB700   | 0.015                           | 0.052                       | 17.19                                | 0.996 |
| DBP-DEHP | B900    | 0.012                           | 0.039                       | 18.64                                | 0.998 |
| DBP-DEHP | AB900   | 0.018                           | 0.043                       | 22.09                                | 0.994 |

between DBP and DEHP in their adsorption to biochar. The studied biochar was more favorable to adsorb DEHP compared with DBP, especially at high PAEs loadings. Apparently, in a binary PAEs system with high PAEs concentration, the accessible adsorption sites on biochar were preferentially occupied by DEHP, contributing to DBP adsorption inhibition. In contrast, the adsorption of DEHP was only marginally inhibited. The two component Langmuir model was applied to the binary DBP-DEHP system (Fig. 2b and d, Table 3). Adsorption isotherms for the binary systems could be well fitted by the two component Langmuir model with relatively high  $R^2$

(0.98–0.99). This suggested that DBP and DEHP adsorption by biochar was a monolayer adsorption procedure. An adsorption site could not be occupied simultaneously by two PAEs (Ni et al., 2019), and competitive adsorption between DBP and DEHP occurred when they coexisted.

### 3.3. Adsorption kinetics of mono and binary PAEs

The effect of contact time on the adsorption of PAEs on B700, B900, AB700, and AB900 in the mono and binary component systems was shown in Fig. 3. In the mono component systems, the adsorption rate was high for both DBP and DEHP during the first 1 h, then it became slower, and the adsorption equilibrium was progressively reached at around 24 h (Fig. 3a and c). The adsorption became less fast in the binary system and reached equilibrium after 48 h (Fig. 3b and d).

To further understand DBP and DEHP's adsorption actions, the adsorption kinetics were analyzed using the pseudo-first-order model and the pseudo-second-order model. All models and the parameters were presented in Supplementary Material S3.

Both kinetic models were used for the kinetic experimental data fitting (Fig. 3), and the parameters and  $R^2$  obtained for the mono and binary PAEs systems were presented in Table S1. The experimental results could be fitted with the pseudo-first-order and pseudo-second-order kinetic models in both the mono and binary component systems. The quality of fit was somewhat better for the pseudo-second-order model ( $R^2 = 0.93–0.99$ ) than for the pseudo-first-order model ( $R^2 = 0.84–0.99$ ). According to the parameters of both the pseudo-first-order and pseudo-second-order models, under the experimental condition, the adsorbed amounts ( $Q_e$ ) of DBP and DEHP were relatively large on the oxidized biochar than on the fresh biochar, and the adsorbed amounts were higher for DEHP than for DBP on the same biochar. These results were in agreement

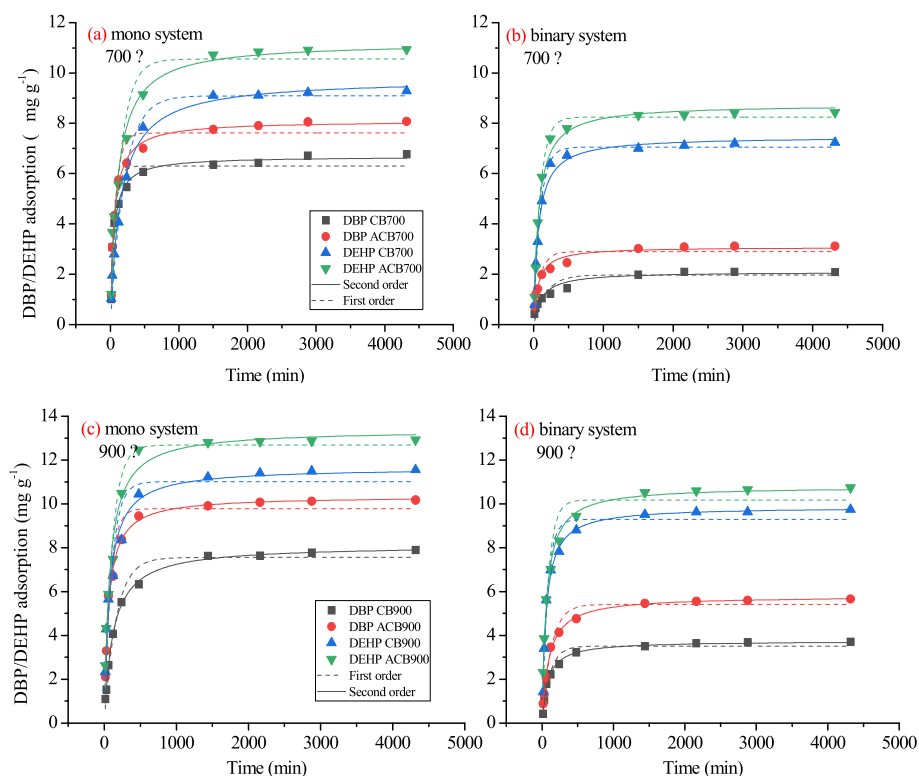


**Fig. 3.** Adsorption kinetics of DBP and DEHP under mono (a, c) and binary (b, d) conditions.

**Table 4**  
Thermodynamic parameters for the adsorption of DBP and DEHP on biochar.

| Biochar | T/K   | lnK <sub>L</sub> | ΔG(kJ mol <sup>-1</sup> ) | ΔH(kJ mol <sup>-1</sup> ) | ΔS(kJ mol <sup>-1</sup> K <sup>-1</sup> ) |       |
|---------|-------|------------------|---------------------------|---------------------------|-------------------------------------------|-------|
| DBP     | B700  | 288              | 8.02                      | -19.2                     | 35.9                                      | 0.191 |
|         |       | 298              | 8.33                      | -20.7                     |                                           |       |
|         |       | 308              | 8.99                      | -23.0                     |                                           |       |
|         | AB700 | 288              | 8.19                      | -19.6                     | 33.4                                      | 0.183 |
|         |       | 298              | 8.46                      | -21.0                     |                                           |       |
|         |       | 308              | 9.09                      | -23.3                     |                                           |       |
| B900    | 288   | 8.11             | -19.4                     | 37.4                      | 0.197                                     |       |
|         | 298   | 8.51             | -21.1                     |                           |                                           |       |
|         | 308   | 9.12             | -23.4                     |                           |                                           |       |
|         | 288   | 8.33             | -20.0                     |                           |                                           |       |
| AB900   | 298   | 8.84             | -21.9                     | 34.3                      | 0.188                                     |       |
|         | 308   | 9.26             | -23.7                     |                           |                                           |       |
|         | 288   | 8.45             | -20.2                     |                           |                                           |       |
| DEHP    | B700  | 298              | 9.43                      | -23.4                     | 39.4                                      | 0.253 |
|         |       | 308              | 9.88                      | -25.3                     |                                           |       |
|         |       | 288              | 8.86                      | -21.2                     |                                           |       |
|         | AB700 | 298              | 9.46                      | -23.5                     | 38.4                                      | 0.207 |
|         |       | 308              | 9.90                      | -25.4                     |                                           |       |
|         | B900  | 288              | 8.80                      | -21.1                     | 41.1                                      | 0.219 |
| 298     |       | 9.52             | -23.6                     |                           |                                           |       |
| 308     |       | 9.91             | -25.4                     |                           |                                           |       |
| AB900   | 288   | 8.85             | -21.2                     | 40.4                      | 0.214                                     |       |
|         | 298   | 9.58             | -23.7                     |                           |                                           |       |
|         | 308   | 9.99             | -25.5                     |                           |                                           |       |

with those observed in the adsorption isotherms. Based on the pseudo-first-order model, the adsorption was faster for DBP than for DEHP except on B900. And Fig. 3 showed that DBP adsorption required less time to reach equilibrium compared to DEHP adsorption. For DBP, the adsorption was faster on (A)B700 than on (A)B900, whereas it was the opposite for DEHP (Table S1). In the presence of other PAEs, DBP adsorption was slowed down except for B900, whereas the adsorption of DEHP became faster on (A) B700 and slower on (A)B900. The differences between the adsorption rate were primarily due to the differences in the biochar properties (Bogusz et al., 2015) and the structure and properties of PAEs (Chen et al., 2019).

### 3.4. Adsorption thermodynamics

To further elucidate the adsorption process, the thermodynamics of PAEs adsorption on biochar were examined. The values for standard enthalpy ( $\Delta H^0$ ), entropy ( $\Delta S^0$ ), and Gibbs free energy ( $\Delta G^0$ ) were calculated using the equations below:

$$\Delta G^0 = -RT \ln K_L \quad (\text{Eq. 2})$$

$$\ln K_L = -\frac{\Delta G^0}{RT} = -\frac{\Delta H^0}{RT} + \frac{\Delta S^0}{R} \quad (\text{Eq. 3})$$

where  $R$  is the gas constant (8.314 J mol<sup>-1</sup> K<sup>-1</sup>),  $T$  is the absolute temperature (K),  $K_L$  is the Langmuir constant (L mol<sup>-1</sup>),  $\Delta H^0$  is the enthalpy change (J mol<sup>-1</sup>), and  $\Delta S^0$  is the entropy change (J mol<sup>-1</sup> K<sup>-1</sup>).  $\Delta H^0$  and  $\Delta S^0$  can be calculated from the plot of  $\Delta G^0$  versus  $T$ . Adsorption isotherm data of DBP and DEHP adsorption to the biochars at pH 7 and at 288 K, 298 K, and 308 K (Figure S3) were used to derive these parameters.

All calculated thermodynamic parameters for DBP and DEHP were shown in Table 4. The adsorption of DBP and DEHP on B700, B900, and AB700, AB900 increased with increasing temperature (maximum adsorption 5.8–11.8 mg g<sup>-1</sup> for DBP and 8.5–13.6 mg g<sup>-1</sup> for DEHP) (Figure S3, Table 4). As revealed in

Table 4, the negative  $\Delta G^0$  values showed that DBP and DEHP adsorption on B700, B900, and AB700, AB900 was a spontaneous process. The decline of  $\Delta G^0$  values with increasing temperature revealed that the adsorption of DBP and DEHP on the biochar was favored at a higher temperature. The positive  $\Delta H^0$  values (Table 4) indicated that DBP and DEHP adsorption on B700, B900, and AB700, AB900 was an endothermic process, which could be attributed to interface water disruption on the surface of biochar (Yang et al., 2011). The positive  $\Delta S^0$  values (Table 4) revealed that the adsorption of DBP and DEHP on biochar was within a dissociative system ( $\Delta S^0 > -10$  kJ mol<sup>-1</sup> K<sup>-1</sup>) (Hu et al., 2017). Therefore, the adsorption of DBP and DEHP on B700, B900, AB700, and AB900 was a spontaneous and endothermic process driven by entropy change according to the thermodynamic parameters calculated (Zhao et al., 2011).

## 4. Discussion

From the results of both mono component and binary component systems, it showed that the DEHP adsorbed more strongly than DBP on the biochar. In the binary systems, DBP adsorption was considerably reduced compared to DEHP, demonstrating competitive adsorption between them and showing the preference of the studied biochar on DEHP over DBP. As indicated by previous studies, the primary mechanism of PAEs sorption to biochar was hydrophobic interaction (Ghaffar and Abbas, 2016). Meanwhile, the  $\pi$ - $\pi$  electron donor-acceptor (EDA) interactions was also proposed as an essential mechanism for the adsorption of chemicals having benzene rings. And H-bonds could also form between the -OH group of biochar and the C=O group of PAEs. As shown in Table 1, the octanol-water partition coefficient ( $\log K_{ow}$ ) increased from 4.61 for DBP to 7.5 for DEHP, indicating a higher hydrophobicity for DEHP (Tang et al., 2015); meanwhile, the water solubility was much higher for DBP (11.2 mg L<sup>-1</sup>) than for DEHP (0.003 mg L<sup>-1</sup>). Thus, the stronger hydrophobic interactions could render stronger adsorption of DEHP onto biochar than DBP. In addition to the adsorption isotherms collected at pH 7, the effects of pH (3.0–10.0) on the adsorption of DBP and DEHP to fresh and oxidized biochar were investigated in this study (Figure S4). It was shown that pH had no significant impact on each biochar's sorption capacity for DBP and DEHP. The lack of pH dependency in the adsorption is in line with hydrophobic adsorption.

Although the adsorbed amount was higher for DEHP than for DBP, a faster adsorption rate for DBP than for DEHP except on B900 was observed based on the pseudo-first-order fitting. The structural configuration of biochar would potentially alter the contact mechanisms and kinetics of organic pollutant's adsorption significantly (Ren et al., 2018) and led to different adsorption rates of DBP and DEHP on biochar. Moreover, the faster rate in adsorption for DBP could also be attributed to its smaller size and shorter chains than DEHP (Table 1), which could have resulted in a faster diffusion of the DBP molecules into the pores of biochar.

To explore the effects of biochar surface properties, i.e., specific surface area, in adsorption of PAEs, the adsorption of DBP and DEHP on fresh and oxidized biochar was normalized to the specific surface area (mg/m<sup>2</sup>) to eliminate the surface area effect (Figure S5). The adsorption amount expressed as per unit of surface area was higher with fresh biochar than oxidized one, and this effect was more evident for DEHP than for DBP and at higher concentrations. As discussed above, when expressed as per unit of mass, the adsorbed amounts of both DEHP and DBP were higher on the oxidized biochar than fresh one. This indicated that the increase of specific surface area might have contributed to the increased adsorption of DBP and DEHP (per unit of mass) on oxidized biochar.

However, the specific surface area was not the only factor determining DBP and DEHP adsorption to biochar. As mentioned above, under the same condition, the adsorption expressed as per unit of surface area was higher on the fresh biochar than on the oxidized biochar. From the elemental composition of the biochar (Table 2), the O/C and (N + O)/C ratios increased after oxidation, which indicated that the hydrophobicity of the surface of biochar decreased after oxidation. If hydrophobic interaction plays an essential role in the adsorption, the decrease of surface hydrophobicity might have led to a decrease of adsorption expressed as per unit of surface area. The decrease of adsorption expressed as per unit surface area was more substantial for DEHP than for DBP, suggesting that hydrophobic interaction is more important for DEHP's adsorption than for DBP.

As revealed by the thermodynamic results, DBP and DEHP sorption on biochar was an endothermic process. In an aqueous solution, DBP and DEHP, as well as the surface of biochar, were well solvated with water molecules arranged on their surfaces via H bonds. For DBP and DEHP to adsorb on biochar by hydrophobic interactions, they must have their hydration sheath denuded to some extent (Fontecha-Camara et al., 2006; Tong et al., 2019), and this dehydration process needed energy. Although weak intermolecular forces, such as H-bonds and  $\pi$ - $\pi$  interactions, might be involved in the adsorption, the endothermic energy of dehydration exceeded the exothermicity of DBP and DEHP in attaching to biochar by H-bonds and/or  $\pi$ - $\pi$  interactions, indicating that hydrophobic interactions were dominated. Also, as dehydration occurred, the orderly arranged water molecules on the biochar surface were displaced. They became disordered, leading to increased entropy, thus reducing the system's free energy to obtain a more stable state, as observed in this study (Table 4). As previous research indicated, hydrophobic interactions between adsorbent and adsorbate were primarily driven by the adsorption system's tendency to gain entropy (Chen et al., 2012; Tong et al., 2019). The gain in entropy denoted nonspecific hydrophobic interactions between the organic molecules and the biochar surface (Meyer et al., 2006). Compared to the mono component system with DBP, higher positive  $\Delta S^0$  and  $\Delta H^0$  values observed in DEHP adsorption further indicated a relatively stronger hydrophobic interaction and weaker H-bonds and  $\pi$ - $\pi$  interactions for DEHP than for DBP (Kah et al., 2017).

## 5. Conclusion

Fresh and chemically oxidized corncob biochar was produced and used to investigate DBP and DEHP's competitive adsorption to biochar in the aqueous environment. In the mono PAEs systems, all the biochar (B700, B900, AB700, and AB900) showed a much higher adsorption capacity for DEHP than for DBP, while DBP exhibited a faster adsorption rate than that of DEHP. The higher hydrophobicity of DEHP could explain the stronger adsorption of DEHP than DBP. In contrast, DBP's faster adsorption could be attributed to its smaller size and shorter chains, therefore faster diffusion. The mass-based adsorption capacity for PAEs was higher with the oxidized biochars than the fresh ones, which could be attributed to the increase of biochar's specific surface area after oxidation.

In the binary PAEs system, DEHP was preferentially adsorbed on biochar, contributing to DBP adsorption inhibition; meanwhile, the adsorption of DEHP was almost marginally inhibited by the presence of DBP. The adsorption isotherms could be well fitted by the two component Langmuir model, indicating a monolayer adsorption procedure. The more hydrophobic DEHP's preference over less hydrophobic DBP suggested that hydrophobic interaction played an essential role in PAEs' adsorption to biochar. The PAEs' adsorption was a spontaneous and endothermic process driven by entropy

change according to the thermodynamic parameters, which confirmed the importance of hydrophobic interactions in the adsorption, while the effects from H-bonds and  $\pi$ - $\pi$  interactions were of secondary importance.

## Declaration of competing interest

The authors declare that they have no known competing financial interests or personal relationships that could have influenced the work reported in this paper.

## Acknowledgments

This research is supported by the National Natural Science Foundation of China (41701355) and the National Key Research and Development Program of China (2017YFD0801003).

## Author contribution statement

Abdoul Salam Issiaka Abdoul Magid: Adsorption material preparation, Methodology, laboratory experiment performance, Formal analysis, and Writing – original draft. Md. Shafiqul Islam: Adsorption material preparation, laboratory experiment performance, Writing – review & editing. Yali Chen: Conceptualization, Methodology, Writing – review & editing, Funding acquisition. Liping Weng: Methodology, Writing – review & editing. Yang Sun: PAEs analysis, Writing – review & editing. Xingping Chang: PAEs analysis, Writing – review & editing. Bin Zhou: Writing – review & editing. Jie Ma: Writing – review & editing. Yongtao Li: Writing – review & editing. All authors contributed substantially to revisions.

## Appendix A. Supplementary data

Supplementary data to this article can be found online at <https://doi.org/10.1016/j.chemosphere.2021.130639>.

## References

- Ahmad, M., Rajapaksha, A.U., Lim, J.E., Zhang, M., Bolan, N., Mohan, D., Vithanage, M., Lee, S.S., Ok, Y.S., 2014. Biochar as a sorbent for contaminant management in soil and water: a review. *Chemosphere* 99, 19–33. <https://doi.org/10.1016/j.chemosphere.2013.10.071>.
- Beesley, L., Moreno-Jiménez, E., Gomez-Eyles, J.L., Harris, E., Robinson, B., Sizmur, T., 2011. A review of biochars' potential role in the remediation, revegetation and restoration of contaminated soils. *Environ. Pollut.* 159, 3269–3282. <https://doi.org/10.1016/j.envpol.2011.07.023>.
- Bogusz, A., Oleszczuk, P., Dobrowolski, R., 2015. Application of laboratory prepared and commercially available biochars to adsorption of cadmium, copper and zinc ions from water. *Bioresour. Technol.* 196, 540–549. <https://doi.org/10.1016/j.biortech.2015.08.006>.
- Cayuela, M.L., van Zwieten, L., Singh, B.P., Jeffery, S., Roig, A., Sánchez-Monedero, M.A., 2014. Biochar's role in mitigating soil nitrous oxide emissions: a review and meta-analysis. *Agric. Ecosyst. Environ.* 191, 5–16. <https://doi.org/10.1016/j.agee.2013.10.009>.
- Chang, B.V., Yang, C.M., Cheng, C.H., Yuan, S.Y., 2004. Biodegradation of phthalate esters by two bacteria strains. *Chemosphere* 55, 533–538. <https://doi.org/10.1016/j.chemosphere.2003.11.057>.
- Chen, B., Chen, Z., Lv, S., 2011. A novel magnetic biochar efficiently sorbs organic pollutants and phosphate. *Bioresour. Technol.* 102, 716–723. <https://doi.org/10.1016/j.biortech.2010.08.067>.
- Chen, Z., Chen, B., Zhou, D., Chen, W., 2012. Bislute sorption and thermodynamic behavior of organic pollutants to biomass-derived biochars at two pyrolytic temperatures. *Environ. Sci. Technol.* 46, 12476–12483. <https://doi.org/10.1021/es303351e>.
- Chen, Q., Zheng, J., Yang, Q., Dang, Z., Zhang, L., 2019. Effect of carbon chain structure on the phthalic acid esters (PAEs) adsorption mechanism by mesoporous cellulose biochar. *Chem. Eng. J.* 362, 383–391. <https://doi.org/10.1016/j.cej.2019.01.052>.
- Cho, H., Wepasnick, K., Smith, B.A., Bangash, F.K., Fairbrother, D.H., Ball, W.P., 2010. Sorption of aqueous Zn[II] and Cd[II] by multiwall carbon Nanotubes: the relative roles of oxygen-containing functional groups and graphenic carbon. *Am. Chem. Soc.* 26, 967–981. <https://doi.org/10.1021/la902440u>.
- Chung, Y.C., Chen, C.Y., 2009. Competitive adsorption of a phthalate esters mixture

- by chitosan bead and  $\alpha$ -cyclodextrin-linked chitosan bead. *Environ. Technol.* 30, 1343–1350. <https://doi.org/10.1080/09593330902858914>.
- Dong, H., Deng, J., Xie, Y., Zhang, C., Jiang, Z., Cheng, Y., Hou, K., Zeng, G., 2017. Stabilization of nanoscale zero-valent iron (nZVI) with modified biochar for Cr(VI) removal from aqueous solution. *J. Hazard Mater.* 332, 79–86. <https://doi.org/10.1016/j.jhazmat.2017.03.002>.
- Fontecha-Camara, M., Lopez-Ramon, M., Alvarez-Merino, A., Moreno-Castilla, C., 2006. About the endothermic nature of the adsorption of the herbicide diuron from aqueous solutions on activated carbon fiber. *Carbon N. Y.* 44, 2330–2356. <https://doi.org/10.1016/j.carbon.2006.05.031>.
- Foster, P.M.D., Cattley, R.C., Mylchreest, E., 2000. Effects of Di-n-butyl phthalate (DBP) on male reproductive development in the rat: implications for human risk assessment. *Food Chem. Toxicol.* 38, 97–99. [https://doi.org/10.1016/s0278-6915\(99\)00128-3](https://doi.org/10.1016/s0278-6915(99)00128-3).
- Gan, C., Liu, Y., Tan, X., Wang, S., Zeng, G., Zheng, B., Li, T., Jiang, Z., Liu, W., 2015. Effect of porous zinc-biochar nanocomposites on Cr(VI) adsorption from aqueous solution. *RSC Adv.* 5, 35107–35115. <https://doi.org/10.1039/c5ra04416b>.
- Gao, B., Wang, P., Zhou, H., Zhang, Z., Wu, F., Jin, J., Kang, M., Sun, K., 2013. Sorption of phthalic acid esters in two kinds of landfill leachates by the carbonaceous sorbents. *Bioresour. Technol.* 136, 295–301. <https://doi.org/10.1016/j.biortech.2013.03.026>.
- German, S., 2014. Les phtalates. (Memoire DESS), Univ. du Quebec a Chicoutimi. Retrieved from. <https://www.uqac.ca/cosmetologie/wp-content/uploads/2015/09/>.
- Ghaffar, A., Abbas, G., 2016. Adsorption of phthalic acid esters (PAEs) on chemically aged biochars. 5. De Gruyter, pp. 407–417. <https://doi.org/10.1515/gps-2016-0014>.
- Ghaffar, A., Ghosh, S., Li, F., Dong, X., Zhang, D., Wu, M., Li, H., Bo, P., 2015. Effect of biochar aging on surface characteristics and adsorption. *Environ. Pollut.* 206, 502–509. <https://doi.org/10.1016/j.envpol.2015.08.001>.
- Ghaffar, A., Zhu, X., Chen, B., 2017. Structural characteristics of biochar-graphene nanosheet composites and their adsorption performance for phthalic acid esters. *Chem. Eng. J.* 319, 9–20. <https://doi.org/10.1016/j.cej.2017.02.074>.
- He, L., Fan, S., Müller, K., Hu, G., Huang, H., Zhang, X., Lin, X., Che, L., Wang, H., 2016. Biochar reduces the bioavailability of di- (2-ethylhexyl) phthalate in soil. *Chemosphere* 142, 24–27. <https://doi.org/10.1016/j.chemosphere.2015.05.064>.
- Herath, I., Kumarathilaka, P., Al-Wabel, M.L., Abduljabbar, A., Ahmad, M., Usman, A.R.A., Vithanage, M., 2016. Mechanistic modeling of glyphosate interaction with rice husk derived engineered biochar. *Microporous Mesoporous Mater.* 225, 280–288. <https://doi.org/10.1016/j.micromeso.2016.01.017>.
- Hu, B., Hu, Q., Xu, D., Chen, C., 2017. The adsorption of U(VI) on carbonaceous nanofibers: a combined batch, EXAFS and modeling techniques. *Separ. Purif. Technol.* 175, 140–146. <https://doi.org/10.1016/j.seppur.2016.11.025>.
- Huang, D., Liu, L., Zeng, G., Xu, P., Huang, C., Deng, L., Wang, R., Wan, J., 2017. The effects of rice straw biochar on indigenous microbial community and enzymes activity in heavy metal-contaminated sediment. *Chemosphere* 174, 545–553. <https://doi.org/10.1016/j.chemosphere.2017.01.130>.
- Jeffery, S., Verheijen, F.G.A., van der Velde, M., Bastos, A.C., 2011. A quantitative review of the effects of biochar application to soils on crop productivity using meta-analysis. *Agric. Ecosyst. Environ.* 144, 175–187. <https://doi.org/10.1016/j.agee.2011.08.015>.
- Jin, J., Sun, K., Wu, F., Gao, B., Wang, Z., Kang, M., Bai, Y., Zhao, Y., Liu, X., Xing, B., 2014. Single-solute and bi-solute sorption of phenanthrene and dibutyl phthalate by plant- and manure-derived biochars. *Sci. Total Environ.* 473–474, 308–316. <https://doi.org/10.1016/j.scitotenv.2013.12.033>.
- Jin, J., Sun, K., Wang, Z., Han, L., Pan, Z., Wu, F., Liu, X., Zhao, Y., Xing, B., 2015. Characterization and phthalate esters sorption of organic matter fractions isolated from soils and sediments. *Environ. Pollut.* 206, 24–31. <https://doi.org/10.1016/j.envpol.2015.06.031>.
- Jing, F., Sohi, S.P., Liu, Y., Chen, J., 2018. Insight into mechanism of aged biochar for adsorption of PAEs: reciprocal effects of ageing and coexisting Cd<sup>2+</sup>. *Environ. Pollut.* 242, 1098–1107. <https://doi.org/10.1016/j.envpol.2018.07.124>.
- Kah, M., Sigmund, G., Xiao, F., Hofmann, T., 2017. Sorption of ionizable and ionic organic compounds to biochar, activated carbon and other carbonaceous materials. *Water Res.* 124, 673–692. <https://doi.org/10.1016/j.watres.2017.07.070>.
- Kookana, R.S., 2010. The role of biochar in modifying the environmental fate, bioavailability, and efficacy of pesticides in soils: a review. *Aust. J. Soil Res.* 48, 627–637. <https://doi.org/10.1071/SR10007>.
- Li, X., Zhong, M., Xu, S., Sun, C., 2006. Determination of phthalates in water samples using polyaniline-based solid-phase microextraction coupled with gas chromatography. *J. Chromatogr.* 1135, 101–108. <https://doi.org/10.1016/j.chroma.2006.09.051>.
- Liu, X., Zhang, Yang, Li, Z., Feng, R., Zhang, Yaozhong, 2014. Characterization of corn-cob-derived biochar and pyrolysis kinetics in comparison with corn stalk and sawdust. *Bioresour. Technol.* 170, 76–82. <https://doi.org/10.1016/j.biortech.2014.07.077>.
- Lu, Y., Tang, F., Wang, Y., Zhao, J., Zeng, X., Luo, Q., Wang, L., 2009. Biodegradation of dimethyl phthalate, diethyl phthalate and di-n-butyl phthalate by *Rhodococcus* sp. L4 isolated from activated sludge. *J. Hazard Mater.* 168, 938–943. <https://doi.org/10.1016/j.jhazmat.2009.02.126>.
- Lu, K., Yang, X., Gielen, G., Bolan, N., Sik, Y., Khan, N., Xu, S., Yuan, G., Chen, X., Zhang, X., Liu, D., Song, Z., Liu, X., Wang, H., 2017. Effect of bamboo and rice straw biochars on the mobility and redistribution of heavy metals (Cd, Cu, Pb and Zn) in contaminated soil. *J. Environ. Manag.* 186, 285–292. <https://doi.org/10.1016/j.jenvman.2016.05.068>.
- Meyer, E.E., Rosenberg, K.J., Israelachvili, J., 2006. Recent progress in understanding hydrophobic interactions. *Proc. Natl. Acad. Sci. Unit. States Am.* 103, 15739–15746.
- Ni, B.J., Huang, Q.S., Wang, C., Ni, T.Y., Sun, J., Wei, W., 2019. Competitive adsorption of heavy metals in aqueous solution onto biochar derived from anaerobically digested sludge. *Chemosphere* 219, 351–357. <https://doi.org/10.1016/j.chemosphere.2018.12.053>.
- Peijnenburg, W.J.G.M., Struijs, J., 2006. Occurrence of phthalate esters in the environment of The Netherlands. *Ecotoxicol. Environ. Saf.* 63, 204–215. <https://doi.org/10.1016/j.ecoenv.2005.07.023>.
- Qian, L., Chen, B., 2013. Dual role of biochars as adsorbents for aluminum: the effects of oxygen-containing organic components and the scattering of silicate particles. *Environ. Sci. Technol.* 47, 8759–8768. <https://doi.org/10.1021/es401756h>.
- Qin, P., Wang, H., Yang, X., He, L., Müller, K., Tsang, D.C.W., Sik, Y., Shaheen, S.M., Xu, S., Bolan, N., Song, Z., Che, L., Xu, X., 2018. Bamboo- and pig-derived biochars reduce leaching losses of dibutyl phthalate, cadmium, and lead from co-contaminated soils. *Chemosphere* 198, 450–459. <https://doi.org/10.1016/j.chemosphere.2018.01.162>.
- Qureshi, U.A., Gubbuk, I.H., Ersoz, M., Solangi, A.R., Taqvi, S.I.H., Memon, S.Q., 2016. A comparative study and evaluation of magnetic and nonmagnetic hydrogels towards mitigation of di butyl and di ethyl hexyl phthalate from aqueous solutions. *J. Taiwan Inst. Chem. Eng.* 59, 578–589. <https://doi.org/10.1016/j.jtice.2015.09.015>.
- Ren, X., Wang, F., Zhang, P., Guo, J., Sun, H., 2018. Aging effect of minerals on biochar properties and sorption capacities for atrazine and phenanthrene. *Chemosphere* 206, 51–58. <https://doi.org/10.1016/j.chemosphere.2018.04.125>.
- Sánchez-García, M., Alburquerque, J.A., Sánchez-Monedero, M.A., Roig, A., Cayuela, M.L., 2015. Biochar accelerates organic matter degradation and enhances N mineralisation during composting of poultry manure without a relevant impact on gas emissions. *Bioresour. Technol.* 192, 272–279. <https://doi.org/10.1016/j.biortech.2015.05.003>.
- Staples, C.A., Peterson, D.R., Parkerton, T.F., Adams, W.J., 1997. The environmental fate of phthalate esters: a literature review. *Chemosphere* 35, 667–749. [https://doi.org/10.1016/S0045-6535\(97\)00195-1](https://doi.org/10.1016/S0045-6535(97)00195-1).
- Tang, X., Suyu, W., Yang, Y., Ran, T., Yunv, D., Dan, A., Li, L., 2015. Removal of six phthalic acid esters (PAEs) from domestic sewage by constructed wetlands. *Chem. Eng. J.* 275, 198–205. <https://doi.org/10.1016/j.cej.2015.04.029>.
- Tong, Y., Mayer, B.K., Mcnamara, P.J., 2019. Adsorption of organic micropollutants to biosolids-derived biochar: estimation of thermodynamic parameters. *Environ. Sci. Water Res. Technol.* 5, 1132–1144. <https://doi.org/10.1039/c8ew00854j>.
- Wang, Z., Zheng, H., Luo, Y., Deng, X., Herbert, S., Xing, B., 2013. Characterization and influence of biochars on nitrous oxide emission from agricultural soil. *Environ. Pollut.* 174, 289–296. <https://doi.org/10.1016/j.envpol.2012.12.003>.
- Wang, Y., Lu, J., Wu, J., Liu, Q., Zhang, H., Jin, S., 2015. Adsorptive removal of fluoroquinolone antibiotics using bamboo biochar. *Sustainability* 7, 12947–12957. <https://doi.org/10.3390/su70912947>.
- Xiang, L., Wang, X.-D., Chen, X.-H., Mo, C.-H., Li, Y.-W., Li, H., Cai, Q.-Y., Zhou, D.-M., Wong, M.-H., Li, Q.X., 2019. Sorption mechanism, kinetics, and isotherms of di-n-butyl phthalate to different soil particle-size fractions. *J. Agric. Food Chem.* 67, 4734–4745. <https://doi.org/10.1021/acs.jafc.8b06357>.
- Yang, S., Sheng, G., Tan, X., Hu, J., Du, J., Montavon, G., Wang, X., 2011. Determination of Ni(II) uptake mechanisms on morденite surfaces: a combined macroscopic and microscopic approach. *Geochem. Cosmochim. Acta* 75, 6520–6534. <https://doi.org/10.1016/j.gca.2011.08.024>.
- Yang, Z., Chen, F., Tang, Y., Li, S., 2015. Selective adsorption of di(2-ethylhexyl) phthalate by surface imprinted polymers with modified silica gel as functional support. *J. Chem. Soc. Pakistan* 37, 939–949.
- Zhang, G., Zhang, Q., Sun, K., Liu, X., Zheng, W., Zhao, Y., 2011. Sorption of simazine to corn straw biochars prepared at different pyrolytic temperatures. *Environ. Pollut.* 159, 2594–2601. <https://doi.org/10.1016/j.envpol.2011.06.012>.
- Zhang, X., He, L., Sarmah, A.K., Lin, K., Liu, Y., Li, J., Wang, H., 2014. Retention and release of diethyl phthalate in biochar-amended vegetable garden soils. *J. Soils Sediments* 14, 1790–1799. <https://doi.org/10.1007/s11368-014-0929-x>.
- Zhao, G., Li, J., Ren, X., Chen, C., Wang, X., 2011. Few-layered graphene oxide nanosheets as superior sorbents for heavy metal ion pollution management. *Environ. Sci. Technol.* 45, 10454–10462. <https://doi.org/10.1021/es203439v>.
- Zhou, M., Zhang, C., Yuan, Y., Mao, X., Li, Y., Wang, N., Wang, S., Wang, X., 2020. Pinewood outperformed bamboo as feedstock to prepare biochar-supported zero-valent iron for Cr<sup>6+</sup> reduction. *Environ. Res.* 187, 109695. <https://doi.org/10.1016/j.envres.2020.109695>.